DOI: 10.1002/ange.201006449

Porphyrinoids

Oxocyclohexadienylidene-Substituted Subporphyrins**

Shin-ya Hayashi, Jooyoung Sung, Young Mo Sung, Yasuhide Inokuma, Dongho Kim, and Atsuhiro Osuka**

A subporphyrin is a genuine ring-contracted porphyrin that has a 14π electron aromatic system and a bowl-shaped structure. The chemistry of subporphyrins began with the synthesis of tribenzosubporphine in 2006,[1] and the synthesis of *meso*-aryl-substituted subporphyrins was achieved later by two groups independently.[2] Subporphyrins are characterized by distinct aromaticity, a porphyrin-like intense absorption, and green fluorescence. Large effects of *meso*-aryl substituents on the electronic properties of subporphyrin owing to their free rotation have been demonstrated for *meso*-4-aminophenyl-substituted subporphyrins,[3a] *meso*-oligo-1,4-phenyleneethynylene-substituted subporphyrins,[3b] and *meso*-oligo-2,5-thienylene-substituted subporphyrins.[3c] Other chemical modifications, such as peripheral modifications[4a,b] and *meso*-alkyl substitution,[4c] have been also developed. Despite these efforts, the chemistry of subporphyrins still remains at its infant stage, and exploration of novel subporphyrins is highly desirable to expand their chemistry.

meso-Alkenylidenyl-substituted porphyrins hold a unique position in porphyrin chemistry in view of extended conjugation, perturbed absorption spectra,[5a] O_2 reduction systems,[5b,c] solvatochromism,[5d] and anion binding.[5e] In many cases, their structures in solution are uncertain because they exist as a variety of tautomers.[6] For example, 3,5-di-*tert*-butyl-4-hydroxyphenyl-substituted porphyrin is readily oxidized to oxocyclohexadienylidene (OCH)-substituted porphyrin, which has an extended quinonoid conjugated structure.[6] To the best of our knowledge, however, none of *meso*-alkenylidene-substituted subporphyrins has been reported to date. Herein, we present OCH-substituted subporphyrin as the first example of *meso*-alkenylidene-substituted subporphyrin.

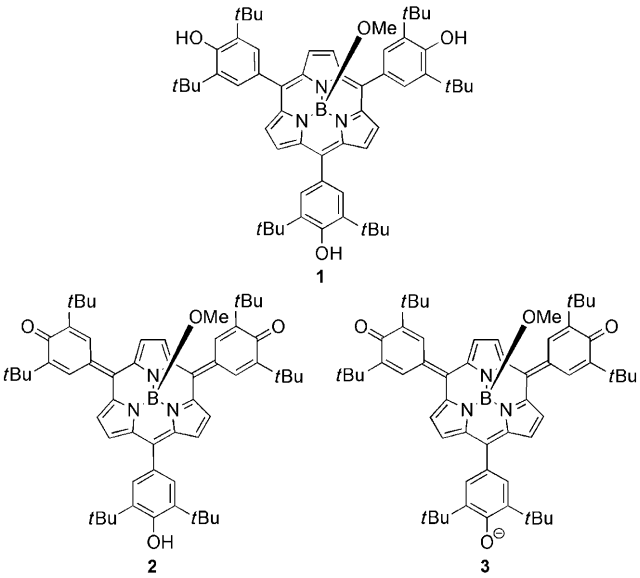

First, we synthesized *meso*-tris(3,5-di-*tert*-butyl-4-hydroxyphenyl)subporphyrin **1** based on the condensation of pyridine-tri-*N*-pyrrolylborane[4b] and 3,5-di-*tert*-butyl-4-hydroxybenzaldehyde with the yield of isolated product being 1.9%. A high-resolution electrospray ionization (HR-ESI) mass measurement revealed an intense borenium cation peak at m/z 855.5446 (calcd for $C_{57}H_{69}B_1N_3O_3 = 855.5436$ $[M-OMe]^+$). The ^1H NMR spectrum had a singlet at $\delta =$ 8.16 ppm for the six β-pyrrolic protons and a single set of signals that are due to the *meso*-aryl substituents, and a singlet at $\delta = 0.90$ ppm for the B-axial methoxy protons. The bowl-shaped structure of **1** was unambiguously confirmed by single-crystal X-ray diffraction analysis (Figure 1).[7] The dihedral angles of the *meso*-aryl substituents towards the subporphyrin core are 34.1°, 48.0°, and 57.6°, respectively, and the bowl depth, defined as the distance from the central boron atom to the mean plane of peripheral six β-carbon atoms, is 1.37 Å. These structural features are common to those of usual *meso*-aryl-substituted subporphyrins.[2a]

Subporphyrin **1** was readily oxidized by MnO_2 to OCH-substituted subporphyrin **2** in 50% yield. It is worth noting that **2** can be reduced to **1** using $NaBH_4$. In contrast to the usual subporphyrin cases, the HR-ESI mass spectrum of **2** did not exhibit a borenium cation peak in the positive-ion mode but displayed a characteristic intense anionic parent peak at m/z 882.5383 (calcd for $C_{58}H_{69}B_1N_3O_4 = 882.5396$ $[M-H]^-$) in the negative-ion mode. The ^1H NMR spectrum of **2** was

[*] S. Hayashi, Dr. Y. Inokuma, Prof. Dr. A. Osuka
Department of Chemistry, Graduate School of Science
Kyoto University, Sakyo-ku, Kyoto 606-8502 (Japan)
Fax: (+81) 75-753-3970
E-mail: osuka@kuchem.kyoto-u.ac.jp
J. Sung, Y. M. Sung, Prof. Dr. D. Kim
Spectroscopy Laboratory for Functional π-Electronic Systems and Department of Chemistry, Yonsei University
Seoul 120-749 (Korea)
Fax: (+82) 2-2123-2434
E-mail: dongho@yonsei.ac.kr

[**] This work was supported by Grants-in-Aid (nos. 22245006 (A) and 20108001 "pi-Space") from MEXT. The work at Yonsei University was supported by World Class University Program (R32-2008-000-10217-0) and the Star Faculty program from the Ministry of Education and Human Resources Development, Korea, and AFSOR/AOARD grant (no. FA 2386-09-1-4092).

Supporting information for this article is available on the WWW under http://dx.doi.org/10.1002/anie.201006449.

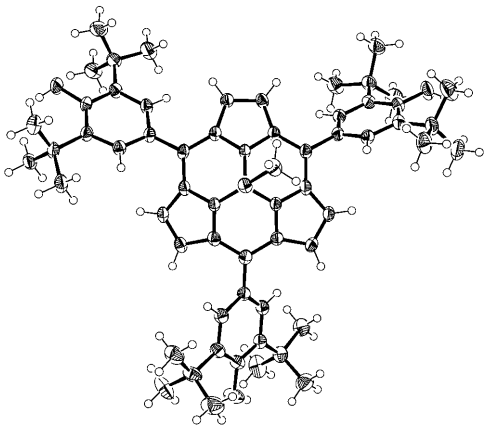

Figure 1. X-ray crystal structure of **1**. Ellipsoids set at 50% probability; solvent molecules are omitted for clarity.

consistent with its non-symmetric structure, differentiating two quinonoidal substituents (two broad singlets at $\delta = 8.33$ and 8.21 ppm) from a hydroxyphenyl substituent (a sharp singlet at $\delta = 7.63$ ppm). The former two broad peaks coalesced at 50 °C, indicating restricted rotation of the quinonoidal substituents or proton transfer among *meso*-substituents. A singlet for the B-axial methoxy protons was observed at $\delta = 2.97$ ppm, indicating dearomatization, which is consistent with the upfield shifts of its β-pyrrolic protons observed at $\delta = 7.20$, 7.11, and 6.87 ppm, respectively.

Single crystals suitable for X-ray diffraction analysis were grown as its B-axial hydroxy derivative **2**-OH (Figure 2) from a solution of **2** in a mixture of acetone/acetonitrile (1:2).[7] The distortion toward the quinonoidal form is obvious as shown in C–O bonds (1.23 and 1.24 Å in the quinonoid moieties, 1.37 Å in the hydroxyphenyl substituent) and C_{meso}–C_{ipso} bonds (1.38 and 1.39 Å in the quinonoid moieties, 1.45 Å in the hydroxyphenyl substituent). Reflecting the quinonoidal structure, the dihedral angles toward the subporphyrin mean plane are quite small (9.5° and 10.1°), but that of the hydroxyphenyl substituent is normal (39.8°). The bowl-shaped structure is preserved, but the pyrrole ring, which is hampered by the two quinonoid substituents, is bent to mitigate the steric congestion, which results in a deeper bowl depth of 1.47 Å. Interestingly, intermolecular hydrogen-bonding interactions between the B-axial hydroxy group and quinone carbonyl, and the B-hydroxy and phenol hydroxy group, are observed in the crystal structure (Supporting Information, Figure S2-2).

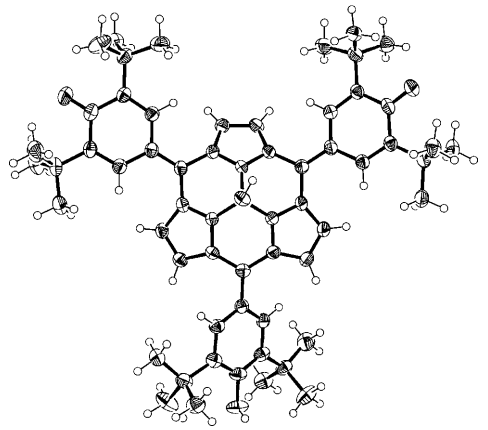

Figure 2. X-ray crystal structure of **2**-OH. Ellipsoids set at 50% probability; solvent molecules are omitted for clarity.

Figure 3 shows UV/Vis absorption and fluorescence spectra of **1** and **2** in CH_2Cl_2. Subporphyrin **1** has absorption and fluorescence spectra that are typical for *meso*-aryl-substituted subporphyrins, with some bathochromic shifts and an enhanced fluorescence quantum yield ($\Phi_F = 0.52$). In sharp contrast, **2** exhibits a remarkably perturbed and red-shifted absorption spectrum that consists of three major bands at 400, 501, and 740 nm, and is virtually non-fluorescent.

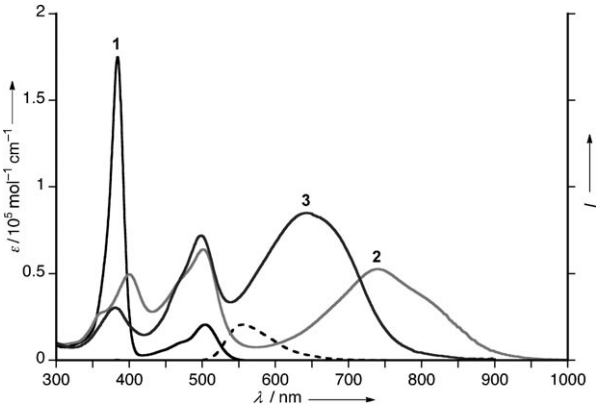

Figure 3. UV/Vis absorption (——) of **1**, **2**, and **3** and fluorescence spectrum of **1** (-----) in CH_2Cl_2.

In the next step, anionic species **3** was generated by the addition of triethylamine (10 equiv) to a solution of **2** in CH_2Cl_2. The color of the solution immediately changed from dark green to blue and the UV/Vis absorption spectrum showed three peaks at 381, 499, and 643 nm (Figure 3). Importantly, the ^{1}H NMR spectrum revealed a C_3-symmetric structure by a singlet at $\delta = 8.20$ ppm for the quinonoidal protons, a singlet at $\delta = 6.85$ ppm for β-pyrrolic protons, a singlet at $\delta = 3.12$ ppm for B-axial methoxy protons, and a singlet at $\delta = 1.44$ ppm for *tert*-butyl protons, indicating its non-aromatic feature and full delocalization of anionic charge over the molecule.

The structure of **3** was unambiguously determined by X-ray diffraction analysis on single crystals of **3**-OH obtained from slow crystallization from a mixture of pyridine/octane (Figure 4).[7] The countercation is a protonated pyridine, which is located just below the bowl of **3**-OH (Supporting Information, Figure S2-3). All *meso* substituents exhibit distinct structural distortions owing to nontrivial contribution of a quinonoidal form. The C–O bond lengths (1.23, 1.24, and 1.26 Å) are in the range of a quinone C–O double bond, and the C_{meso}–C_{ipso} bonds (1.38, 1.40 and 1.40 Å) show double-bond character. The dihedral angles are all small (0.8°, 4.9°, and 6.6°). These structural features give rise to severe bending of all of the pyrrole units to avoid the steric congestion, causing a large bowl depth (1.56 Å). As a whole, the

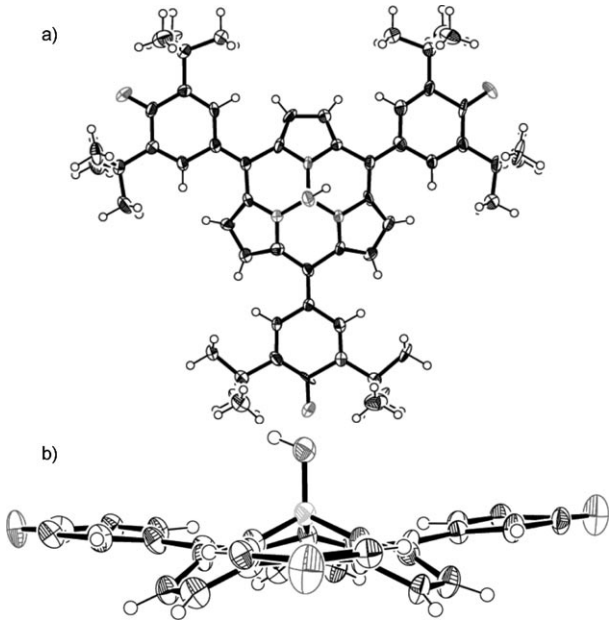

Figure 4. X-ray crystal structure of **3**-OH. a) Top view and b) side view. Ellipsoids set at 50% probability; solvent molecules, counterion, and *tert*-butyl groups are omitted for clarity.

subporphyrin **3**-OH has a planar extended structure with almost C_3 symmetry.

The absorption spectrum of **2** is dependent on solvent polarity: it is red-shifted in nonpolar solvents (dichloromethane, toluene, and hexane) and blue-shifted in polar solvent (methanol, pyridine, and DMSO; Supporting Information, Figure S3-1). Interestingly, the latter spectra are almost the same as that of **3**, suggesting that the subporphyrin **2** exists as a deprotonated species in these polar solvents, as the anion **3** is considerably stabilized owing to the effective delocalization of the negative charge.

To gain further insight into the effect of the OCH substituent on the electronic system, we investigated the excited-state dynamics. Many porphyrinoids with quinonoidal substituents at *meso* positions have short excited-state lifetimes and low fluorescence quantum yields.[5] Specifically, Milgrom et al. have shown that *meso*-tetrakis(3,5-di-*tert*-butyl-4-oxocyclohexadienylidene)porphyrin has a sub-picosecond S_1 state lifetime and low fluorescence quantum yield, while *meso*-tetrakis(3,5-di-*tert*-butyl-4-hydroxyphenyl)porphyrin shows a few nanosecond S_1 state lifetime.[5c,8] Similarly, we observed that quinonoidal subporphyrin system **2** exhibits a short S_1-state lifetime (ca. 40 ps; Supporting Information, Figure S4-1), while *meso*-tris(3,5-di-*tert*-butylphenyl)subporphyrin has a 3 ns lifetime.[4b] Furthermore, even a shorter S_1-state lifetime (ca. 10 ps; Supporting Information, Figure S4-2) is observed for **3**. Owing to the electron-donating ability of the phenoxide anion and coupling between the phenoxide anion and subporphyrin π and π^* molecular orbitals, intramolecular charge transfer occurs in anionic species **3**. These interactions increase electron density over the subporphyrin system and raise the energy of π^* orbital, leading to a blue-shift in the absorption spectra. The promotion of electron density to subporphyrin core by the intramolecular charge-transfer leads to a shorter excited-state lifetime more significantly than neutral species **2**.

The oxidation and reduction potentials of **1**–**3** were measured by cyclic voltammetry in CH_2Cl_2 containing 0.10 M Bu_4NPF_6 as a supporting electrolyte (Supporting Information, Figure S5). Subporphyrin **1** exhibited two oxidation potentials at 0.27 and 0.54 V and one reduction potential at −2.12 V. OCH-substituted subporphyrin **2** exhibited one reversible oxidation wave at 0.55 V and a reduction wave at −1.23 V, while anionic species **3** showed two reversible oxidation waves at 0.10 and 0.58 V, and a reduction wave at −1.22 V. The second reversible oxidation wave of **1** was considered to be identical to the first reversible oxidation wave of **2**. Subporphyrin **2** and **3** showed quite similar reduction waves, which probably arises from the common quinonoidal structure, but anionic species **3** is apparently more susceptible to oxidation. MO calculations on **1**–**3** were performed at the B3LYP/6-31G(d) level (Supporting Information, Figure S6 and S7).[9] Subporphyrin **1** has a_{2u}-like HOMO, a_{1u}-like HOMO−1, and a couple of degenerate e_g-like LUMO and LUMO + 1. Compound **2** has quite similar but stabilized HOMO−1, LUMO + 1, and LUMO + 2 compared to the HOMO−1, LUMO, and LUMO + 1 of **1**, while the HOMO and LUMO of **2** are totally different from the MOs of **1** and have a small energy gap. This observation is consistent with the experimental results. Molecular orbitals of **3** are quite similar to **2**, but characterized by destabilization and delocalization.

In summary, we have synthesized the novel subporphyrin analogue **2** by the oxidation of **1**. OCH-substituted subporphyrin **2** exhibits quite different electronic and structural properties from typical subporphyrins. Deprotonation of **2** proceeds smoothly to provide the anionic species **3** that exhibits an almost planar C_3-symmetric structure. Exploration of more elaborate molecular systems incorporating this switching unit is now being actively pursued in our laboratories.

Received: October 14, 2010
Revised: December 20, 2010
Published online: March 2, 2011

Keywords: conjugated systems · delocalization · oxoporphyrinogen · porphyrinoids · subporphyrins

[1] a) Y. Inokuma, J. H. Kwon, T. K. Ahn, M.-C. Yoon, D. Kim, A. Osuka, *Angew. Chem.* **2006**, *118*, 975–978; *Angew. Chem. Int. Ed.* **2006**, *45*, 961–964; b) T. Torres, *Angew. Chem.* **2006**, *118*, 2900–2903; *Angew. Chem. Int. Ed.* **2006**, *45*, 2834–2837.

[2] a) Y. Inokuma, Z. S. Yoon, D. Kim, A. Osuka, *J. Am. Chem. Soc.* **2007**, *129*, 4747–4761; b) N. Kobayashi, Y. Takeuchi, A. Matsuda, *Angew. Chem.* **2007**, *119*, 772–774; *Angew. Chem. Int. Ed.* **2007**, *46*, 758–760.

[3] a) Y. Inokuma, S. Easwaramoorthi, Z. S. Yoon, D. Kim, A. Osuka, *J. Am. Chem. Soc.* **2008**, *130*, 12234–12235; b) Y. Inokuma, S. Easwaramoorthi, S. Y. Jang, K. S. Kim, D. Kim, A. Osuka, *Angew. Chem.* **2008**, *120*, 4918–4921; *Angew. Chem. Int. Ed.* **2008**, *47*, 4840–4843; c) S. Hayashi, Y. Inokuma, A. Osuka, *Org. Lett.* **2010**, *12*, 4148–4151.

[4] a) E. Tsurumaki, S. Saito, K. S. Kim, J. M. Lim, Y. Inokuma, D. Kim, A. Osuka, *J. Am. Chem. Soc.* **2008**, *130*, 438 – 439; b) E. Tsurumaki, Y. Inokuma, S. Easwaramoorthi, J. M. Lim, D. Kim, A. Osuka, *Chem. Eur. J.* **2009**, *15*, 237 – 247; c) S. Hayashi, Y. Inokuma, S. Easwaramoorthi, K. S. Kim, D. Kim, A. Osuka, *Angew. Chem.* **2010**, *122*, 331 – 334; *Angew. Chem. Int. Ed.* **2010**, *49*, 321 – 324.

[5] a) I. M. Blake, H. L. Anderson, D. Beljonne, J.-L. Brédas, W. Clegg, *J. Am. Chem. Soc.* **1998**, *120*, 10764 – 10765; b) T. G. Traylor, K. B. Nolan, R. Hildreth, *J. Am. Chem. soc.* **1983**, *105*, 6149 – 6151; c) L. R. Milgrom, C. C. Jones, A. Harriman, *J. Chem. Soc. Perkin Trans. 2* **1988**, 71 – 79; d) J. P. Hill, A. L. Schumacher, F. D'Souza, J. Labuta, C. Redshaw, M. R. J. Elsegood, M. Aoyagi, T. Nakanishi, K. Ariga, *Inorg. Chem.* **2006**, *45*, 8288 – 8296; e) A. Shundo, J. P. Hill, K. Ariga, *Chem. Eur. J.* **2009**, *15*, 2486 – 2490.

[6] a) L. R. Milgrom, *Tetrahedron* **1983**, *39*, 3895 – 3898; b) J. P. Hill, I. J. Hewitt, C. E. Anson, A. K. Powell, A. L. McCarry, P. A. Karr, M. E. Zandler, F. D'Souza, *J. Org. Chem.* **2004**, *69*, 5861; c) Y. Xie, J. P. Hill, A. L. Schumacher, P. A. Karr, F. D'Souza, C. E. Anson, A. K. Powell, K. Ariga, *Chem. Eur. J.* **2007**, *13*, 9824 – 9833.

[7] Crystallographic data for **1**: $C_{58}H_{72}B_1N_3O_4 \cdot C_8H_{18}$, $M_r = 1000.22$, monoclinic, space group $P2_1/a$ (no. 14), $a = 18.016(5)$, $b = 18.660(4)$, $c = 19.494(4)$ Å, $\beta = 116.063(9)°$, $V = 5887(2)$ Å^3, $T = 123$ K, $\rho_{calcd} = 1.128$ g cm^{-1}, $Z = 4$, $R_1 = 0.0706$ ($I > 2\sigma(I)$), $R_w = 0.1978$ (all data), GOF = 1.029. **2**: $4(C_{57}H_{68}B_1N_3O_4) \cdot 1.46(C_3H_6O_1) \cdot C_2H_3N_1$, $M_r = 3605.43$, monoclinic, space group $P2_1/a$ (no. 14), $a = 14.919(3)$, $b = 24.058(6)$, $c = 18.377(5)$ Å, $\beta = 114.996(9)°$, $V = 5978(3)$ Å^3, $T = 123$ K, $\rho_{calcd} = 1.002$ g cm^{-1}, $Z = 1$, $R_1 = 0.0824$ ($I > 2\sigma(I)$), $R_w = 0.2130$ (all data), GOF = 1.041. **3**: $2(C_{57}H_{67}B_1N_3O_4) \cdot 2(C_5H_6N_1) \cdot 13(C_5H_5N_1)$, $M_r = 2926.41$, orthorhombic, space group *Ama*2 (no. 40), $a = 29.305(5)$, $b = 18.062(4)$, $c = 31.395(8)$ Å, $V = 16\,618(6)$ Å^3, $T = 123$ K, $\rho_{calcd} = 1.170$ g cm^{-1}, $Z = 4$, $R_1 = 0.0655$ ($I > 2\sigma(I)$), $R_w = 0.1394$ (all data), GOF = 1.003. CCDC 794968 (**1**), 794969 (**2**), and 794970 (**3**) contain the supplementary crystallographic data for this paper. These data can be obtained free of charge from The Cambridge Crystallographic Data Centre via www.ccdc.cam.ac.uk/data_request/cif.

[8] M. A. Bergkamp, J. Dalton, T. L. Netzel, *J. Am. Chem. Soc.* **1982**, *104*, 253 – 259.

[9] See the Supporting Information for the full citation.

